JOURNAL OF VIROLOGY, Oct. 2003, p. 10479–10487 Vol. 77, No. 19
0022-538X/03/$08.00+0 DOI: 10.1128/JVI.77.19.10479–10487.2003

Tissue-Specific Replicating Capacity of a Chimeric Poliovirus That Carries the Internal Ribosome Entry Site of Hepatitis C Virus in a New Mouse Model Transgenic for the Human Poliovirus Receptor

Akiko Yanagiya,[1] Seii Ohka,[1] Noriyasu Hashida,[1] Masahito Okamura,[1] Choji Taya,[2] Nobuhiko Kamoshita,[1]† Kuniko Iwasaki,[3] Yukari Sasaki,[3] Hiromichi Yonekawa,[2] and Akio Nomoto[1]*

Department of Microbiology, Graduate School of Medicine, The University of Tokyo, Bunkyo-ku, Tokyo 113-0033,[1] Department of Laboratory Animal Science, Tokyo Metropolitan Institute of Medical Science, Bunkyo-ku, Tokyo 113-8613,[2] and Institute of Medical Science, The University of Tokyo, Minato-ku, Tokyo 108-8639,[3] Japan

Received 29 April 2003/Accepted 10 July 2003

Nucleotides (nt) 108 to 742 of an infectious cDNA clone of poliovirus (PV) Mahoney strain, including the corresponding region of the internal ribosome entry site (IRES), was replaced by nt 28 to 710 of hepatitis C virus (HCV) cDNA corresponding to the whole HCV IRES. A chimeric PV (2A-369) was generated by transfecting mammalian cells with an RNA transcribed in vitro from the cDNA. To examine replicating capacity of virus 2A-369 in the brain and liver of a mouse model for poliomyelitis, a new mouse model (MPVRTg25-61) that is transgenic for human PV receptor (hPVR; CD155) was generated in order to obtain a higher expression level of hPVR in the liver than those of hPVRTg mouse lines generated by us so far. The transgene used was constructed by combining a putative regulatory region of the mouse PVR homolog and the whole structural region of the hPVR gene. Virus 2A-369 replicated well in the liver of MPVRTg25-61 but not in the brain, whereas control Mahoney virus replicated well both in the liver and in the brain. The data suggest that the HCV IRES works more efficiently in the liver than in the brain and that PV IRES works well both in the liver and in the brain. The results support the notion that tissue-specific activity of IRES may be reflected in tissue tropism of a virus whose specific translation initiation is driven by IRES, that is, an IRES-dependent virus tropism.

Internal initiation of translation for eukaryotic mRNAs was first described for picornavirus RNAs such as poliovirus (PV) RNA (27) and encephalomyocarditis virus RNA (12). Since then, an internal ribosome entry site (IRES) has been discovered on many cellular mRNAs (37), as well as other viral RNAs, including hepatitis C virus (HCV) RNA (36, 38). Nucleotide sequences that serve as IRESs discovered thus far have a variety of lengths and predicted secondary structures, although all of them have similar functions in translation initiation. This observation suggests that individual IRESs require different sets of *trans*-acting cellular factors to initiate translation. In fact, the translation of PV RNA does not occur efficiently in a cell-free translation system of rabbit reticulocyte lysates (RRL), although other IRESs, such as the IRESs of encephalomyocarditis virus RNA (12) and HCV RNA (36), are highly functional in the RRL. The poor translation of PV RNA in RRL is markedly improved by the addition of factors from HeLa cells. Furthermore, it has been reported that PV IRES requires higher concentrations of La protein, one of the *trans*-acting cellular factors, than HCV IRES to display its activity in cell-free translation systems (11). These observations strongly support the notion that cellular factors required for IRES activity are different quantitatively and/or qualitatively in individual IRESs.

* Corresponding author. Mailing address: Department of Microbiology, Graduate School of Medicine, The University of Tokyo, 7-3-1 Hongo, Bunkyo-ku, Tokyo 113-0033, Japan. Phone: 81-3-5841-3413. Fax: 81-3-5841-3374. E-mail: anomoto@m.u-tokyo.ac.jp.

† Present address: Department of Biology, Massachusetts Institute of Technology, Cambridge, MA 02139-4307.

PV is the causative agent of poliomyelitis, an acute disease of the central nervous system (CNS). Natural PV infection in humans begins with oral ingestion, and paralytic poliomyelitis occurs as a result of the destruction of neurons induced by the lytic replication of PV. This neurotropic virus is a human enterovirus that belongs to the family *Picornaviridae*. The genome of PV is a single-stranded, positive-strand RNA of ca. 7,500 nucleotides (nt) that encodes a single open reading frame (ORF). A polyprotein translated from the ORF is processed by virus-encoded proteases (20). The PV IRES element spans approximately from nt 100 to 600, and the 5′-proximal 100-nt span, including the 5′-cloverleaf-like structure, is involved in the initiation of viral RNA replication (1).

To control poliomyelitis, attenuated PV strains of all three serotypes have been developed and effectively used as oral live vaccines, that is, Sabin 1 (type 1), Sabin 2 (type 2), and Sabin 3 (type 3). The attenuated strains have a very poor capacity to replicate in the CNS. However, they can replicate to a sufficiently high level to elicit neutralizing antibodies in the human alimentary tract. Thus, the attenuated strains have a tissue tropism different from that of virulent PVs.

An effective mutation of the neurovirulence phenotype of PV was first described for PV type 3 by comparative sequence analysis between the attenuated Sabin 3 and its neurovirulent revertants (6). As a result, nt 472 was revealed to be a neurovirulence determinant. Molecular genetic analysis of the attenuation phenotype of PV type 1 has revealed that a relatively strong determinant of neurovirulence resides in the 5′ untranslated region (UTR) of the viral RNA, particularly at nt 480 (15, 26). A neurovirulence determinant in the PV type 2 genome

has been found at nt 481 (22). These sites exist within the region corresponding to the IRES. If IRES structure determines tissue-specific activity of individual IRESs, it is reasonable that the IRES region regulates the CNS specificity of PV, although there are multiple neurovirulence determinants scattered throughout the PV genomes. In fact, Gromeier et al. (8, 9) have reported that exchange of the PV IRES with its counterpart from human rhinovirus type 2 results in attenuation of neurovirulence in mice transgenic (Tg) for human PV receptor (hPVR; CD155) and primates. Furthermore, Pilipenko et al. (29) have demonstrated, by using the IRES of neurovirulent picornavirus, the GDVII strain of Theiler's murine encephalomyelitis virus, that the tissue-specific expression and differential RNA-binding properties of polypyrimidine tract-binding protein, one of the *trans*-acting cellular factors for IRES activity, are important determinants of cell-specific translational control and viral neurovirulence.

HCV, known to be a main causative agent of non-A, non-B hepatitis (23), is classified into a separate genus of *Flaviviridae*. The genome of HCV consists of a single-stranded, positive-sense RNA of ca. 9,500 nt that encodes a single ORF (14, 19, 34, 35). The viral structural and nonstructural proteins are produced by protein processing of a polyprotein precursor translated from the ORF. The length of the 5′ UTR of HCV RNA is ca. 340 nt, and the 5′-proximal 27-nt region does not appear to be involved in IRES activity (13). The 3′ boundary of HCV IRES is not clearly determined but seems to reside in the ORF sequence corresponding to the core gene (31). Indeed, our unpublished data (N. Kamoshita and A. Nomoto, unpublished data) indicated that HCV RNA nt 28 to 710 showed a maximum IRES activity in a cell-free translation system.

Lu and Wimmer (21) have demonstrated that the IRES of PV can be functionally replaced by the related genetic element of HCV. That study showed that a chimera PV carrying the HCV 5′ UTR and the coding sequence for the N-terminal 123 amino acids of the core protein is most viable among chimera PVs tested. To generate a proper N terminus of the PV structural protein precursor P1, it is necessary to insert PV protease cleavage site at the junction of the HCV core amino acid sequence and the PV P1. Comparison of growth properties between chimera PVs that carry 2A protease ($2A^{pro}$) or 3C protease ($3C^{pro}$) cleavage site revealed that the former chimera grew better than the latter (41).

The availability of a chimeric PV carrying HCV IRES made it possible to examine the replicating capacity of the chimera virus in the liver and the brain. The experiment may prove the notion of IRES-dependent organ tropism of virus. Unfortunately, the expression level of hPVR gene in the liver of the hPVRTg mouse lines that we have generated thus far is extremely low, and it has been difficult to detect hPVR in the liver by Western blotting. A new mouse model must be generated for the experiment to examine the replicating capacity of the chimera PV.

We demonstrate here that the chimeric PV replicates in the liver but not in the brain of a new mouse model Tg for hPVR, whereas control PV Mahoney virus replicates well both in the liver and in the brain. Our results support the notion of IRES-dependent virus tropism.

MATERIALS AND METHODS

Cells and viruses. HeLa S3 monolayer cells were maintained in Dulbecco modified Eagle medium (DMEM) supplemented with 5% newborn calf serum (NCS) and used for transfection experiments and plaque assays.

PV type 1 Mahoney strain and the related chimera PV were produced in HeLa cells transfected with the corresponding RNAs transcribed in vitro from infectious cDNA clones of pOM1 (32) and p2A-369 (an infectious cDNA clone of a chimera PV as described below), respectively. In the case of p2A-369, the cells transfected with p2A-369 were incubated in DMEM containing 1% NCS at 36°C for up to 4 days.

DNA procedure. Mouse PVR homolog (MPH) (24) is the mouse homolog of hPVR-related gene 2 product (PRR2) (2, 5), which belongs to the Nectin family (33). The MPH gene was isolated from the mouse liver gene library in the cosmid pWE15 vector (Stratagene) derived from C57BL/6 mouse line and named clone 9 (Fig. 1). A probe used was a DNA fragment of MPH cDNA (2). Clone 9 (ca. 46 kbp containing ca. 38 kbp of MPH gene) was treated with *Cla*I, self-ligated, and named clone 9-1 (ca. 31 kbp containing ca. 23 kbp of MPH gene). Clone 9-1 was linearized by *Cla*I digestion, partially digested with *Bam*HI, ligated with *Sac*II linker, and circularized. This cosmid clone was designated clone 9-2 (ca. 20 kbp) and contained a sequence of ca. 12 kbp upstream from the MPH structural gene (Fig. 1).

A *Sac*II-linearized cosmid clone 9-2 (ca. 20 kbp), including the MPH regulatory gene of ca. 12 kbp; a *Sac*II-*Sal*I fragment (ca. 30 kbp) of cosmid clone HC5 corresponding to the hPVR structural gene (17); and a PCR product (ca. 700 bp), including the cos sequence, were ligated and packaged by using Gigapack II packaging extract (Stratagene). *Escherichia coli* JM109 cells were infected with the phage particles carrying the cosmid clone of MPH-hPVR fusion (MPVR) gene. Expression of functional hPVR on the cell surface of mouse L cells transfected with the cosmid clone of MPVR gene was confirmed by an immunofluorescence study with an anti-hPVR monoclonal antibody, p286 (39).

For construction of chimeric PV cDNA, nt 108 to 742 of pOM1 (32) were replaced by the 5′ UTR (nt 28 to 341) plus the N-terminal 123 condons of the core ORF of HCV genotype 1b cDNA clone, pC1b (13). A nucleotide sequence encoding $2A^{pro}$ cleavage site, DLTTY∗G (the asterisk denotes a scissile bond), was inserted at the junction of HCV core coding sequence and PV ORF. This chimeric infectious cDNA clone was designated p2A-369, and the virus derived from the cDNA clone was 2A-369 (see Fig. 3), which is similar to a chimeric PV, P/H701-2A (41).

Tg mice. The MPVR cosmid clone was linearized by cutting at *Sal*I sites within the nucleotide sequence on the vector DNA (Fig. 1). The linearized DNA was introduced into the pronuclei of C57BL/6 mouse zygotes (18). Mice were screened for the transgene by PCR to amplify ca. 700 bp within the exon 8 of hPVRα with the primers 5′-CAGGTGCCAAGTTCATAGGT-3′ and 5′-GAA TATCCTGCCTGGTAGCT-3′. As a result, four lines of Tg mice—MPVRTg5, MPVRTg25-61, MPVRTg25-89, and MPVRTg26-13—derived from strain C57BL/6 were established. MPVRTg25-61 was used in the present study. Transgenes in these lines are maintained in the hemizygous stage.

IQI-PVRTg21 (PVRTg21) (25, 39) at the hemizygous stage with the IQI mouse line (inbred strain of ICR mouse) and the non-Tg C57BL/6 mouse line were used as control mouse lines.

All mice used had been maintained under specific-pathogen-free conditions and were treated in strict compliance with guidelines established by the University of Tokyo.

Southern blot analysis. The genomic DNAs were prepared from HeLa S3 cells and the liver of PVRTg21 and MPVRTg25-61 and then digested with *Bam*HI. Next, 10-μg portions of the digests were separated by gel electrophoresis on 0.8% agarose in a buffer containing 400 mM Tris, 400 mM glacial acetic acid, and 10 mM EDTA (pH 8.0) and then transferred onto Hybond-N filter (Amersham Biosciences). A *Hin*dIII-*Bgl*II fragment carrying sequence for the whole translated region of hPVRα was prepared from pSV2PVRα (17), labeled with ^{32}P, and used as a probe.

Western blot analysis. The brains, spinal cords, livers, and small intestines were homogenized in a motor-driven Potter-Elvehjem glass–Teflon homogenizer with a solution A (250 mM sucrose, 1 mM EDTA [pH 7.5], 1 mM PMSF, 10 μg of aprotinin/ml, 5 mM *N*-ethylmaleimide, 10 μg of leupeptin/ml, 20 mM Tris-HCl [pH 7.5]) to prepare 10% emulsions. The crude extracts were centrifuged at 2,000 rpm for 10 min at 4°C to remove debris. The supernatant was centrifuged at 43,000 rpm for 2 h at 4°C in a Beckman TLA-100.3 rotor, and the pellet was suspended in solution A containing 1% Nonidet P-40 at 4°C for 1 h. This suspension was centrifuged again at 43,000 rpm for 2 h at 4°C as described above. The supernatant (15 μg of protein) was separated by 10% polyacrylamide gel electrophoresis in a buffer containing 0.1% sodium dodecyl sulfate (SDS) (2) and

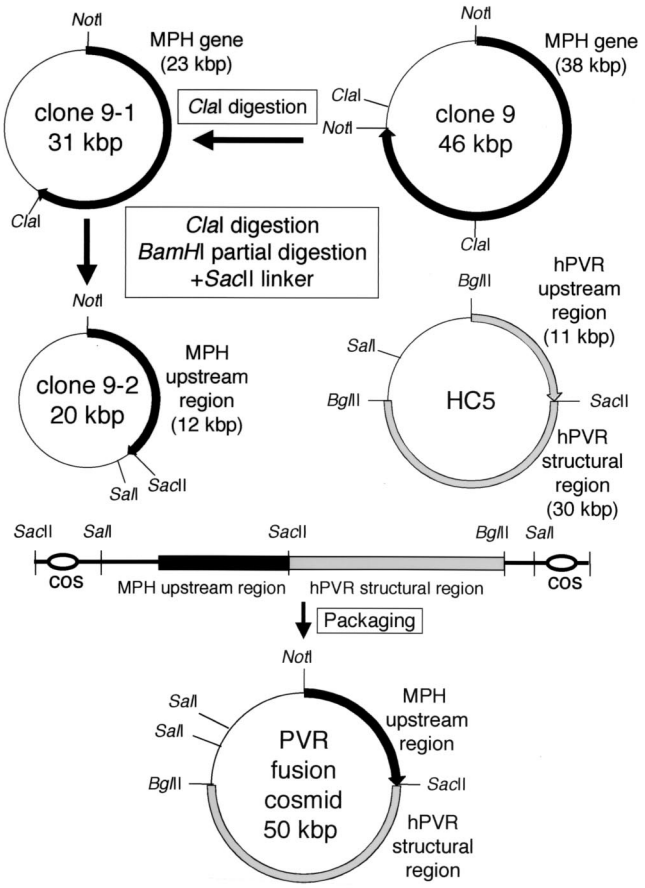

FIG. 1. Construction procedure of a cosmid carrying the fusion gene of MPH upstream region and hPVR structural region.

then transferred onto Immobilon transfer membrane (Millipore). The amount of protein was estimated by using the Bio-Rad protein assay kit (Bio-Rad). The membrane was probed with rabbit anti-hPVR polyclonal antibodies (3) and visualized by using ECL detection reagents (Amersham Biosciences) in accordance with the manufacturer's instructions.

Virus growth in vivo and neurovirulence. A 30- or 5-μl portion of virus suspension containing 10^4 PFU of the Mahoney virus or 2A-369 virus was inoculated directly into the brain (10) or the liver, respectively, of mice anesthetized with an intraperitoneal injection of ca. 300 to 400 μl of 10 mg of ketamine/ml and 0.2 mg of xylazine/ml. The inoculated tissues were removed from the anesthetic mice with chloroform at 0, 12, 24, 48, 72, 96, and 120 h postinfection (hpi) and homogenized as described above in a serum-free DMEM to prepare a 10% emulsion of tissues. The emulsion was centrifuged at 3,000 rpm for 15 min at 4°C to remove debris, and the virus titer of the supernatant was measured by plaque assay.

For the mouse neurovirulence test, anesthetized mice as described above were intracerebrally inoculated with 10^4 PFU of the Mahoney or 2A-369 virus. The mice were observed daily for paralysis and mortality for up to 14 days.

Immunofluorescence study. The mice inoculated with 10^4 PFU of viruses were anesthetized at 96 hpi and perfused with phosphate-buffered saline (PBS; 8 g of NaCl, 0.2 g of KCl, 1.15 g of Na_2HPO_4, and 0.2 g of KH_2PO_4/liter) through the left ventricle. The brain or liver was removed by dissection and frozen immediately in O.C.T. compound (Sakura Finetechnical Co., Ltd.). Tissue sections were prepared by using a Jung CM3000 cryostat (Leica Instruments GmbH), mounted on 3-aminopropyltriethoxysilane-coated slides (Matsunami Glass Ind., Ltd.), and dried at room temperature. Sections were fixed with 2% paraformaldehyde in PBS at room temperature for 10 min and then washed with PBS. The sections were treated with PBS containing 0.5% Triton X-100 at 4°C for 5 min for permeation after the treatment with PBS containing 100 mM glycine at room temperature for 20 min and then washed again with PBS. Nonspecific staining was blocked by treatment with 3% BSA Fraction V (Sigma A-2058) and 0.02% sodium azide in PBS at 37°C for 30 min. The sections were reacted with rabbit hyperimmune serum against PV type 1 at 37°C for 2 h and then treated with goat anti-rabbit immunoglobulin G conjugated with Alexa Fluor 488 (Molecular Probes) at 37°C for 2 h. Nucleic acids were stained with DAPI (4′,6′-diamidino-2-phenylindole). The sections were mounted with 80% (vol/vol) glycerol and analyzed with an inverted microscope DM IRE2 (Leica Microsystems) equipped with a confocal imaging spectrophotometer TCS SP2 (Leica Microsystems).

RESULTS

Tg mice carrying the MPH-hPVR (MPVR) fusion gene. To examine replicating capacity of PV and the related chimeric PV, it is desirable that the expression levels of hPVR in cells of the liver and brain of animal models be sufficiently high to promote the early infection cycle, such as virus binding to cell surface, penetration, and uncoating of the virus. hPVRTg mouse lines that we have generated so far show very low

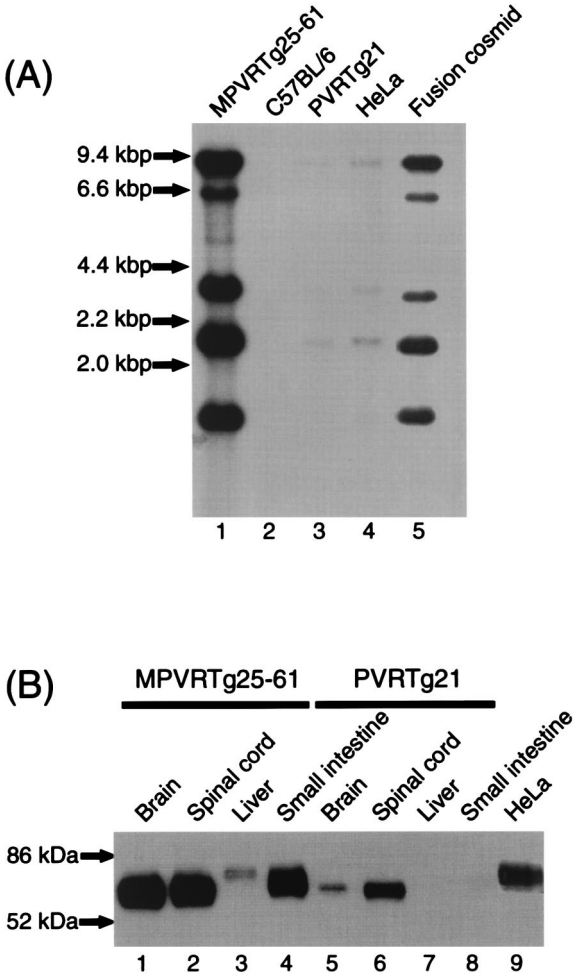

FIG. 2. Detection of transgene and hPVR in Tg mice. (A) Southern blot analysis of *Bam*HI digests of the genomic DNA prepared from the livers of MPVRTg25-61 (lane 1), C57BL/6 (lane 2), and PVRTg21 (lane 3). Similar analysis was performed on the DNA of HeLa cells (lane 4) and chimera cosmid shown in Fig. 1 (lane 5). Experimental conditions are described in Materials and Methods. (B) Western blot analysis of hPVR in MPVRTg25-61 (lanes 1 to 4), PVRTg21 (lanes 5 to 8), and HeLa cells (lane 9). Membrane fractions of various tissues of MPVRTg25-61 and PVRTg21 were prepared, and hPVR in these fractions was detected as described in Materials and Methods.

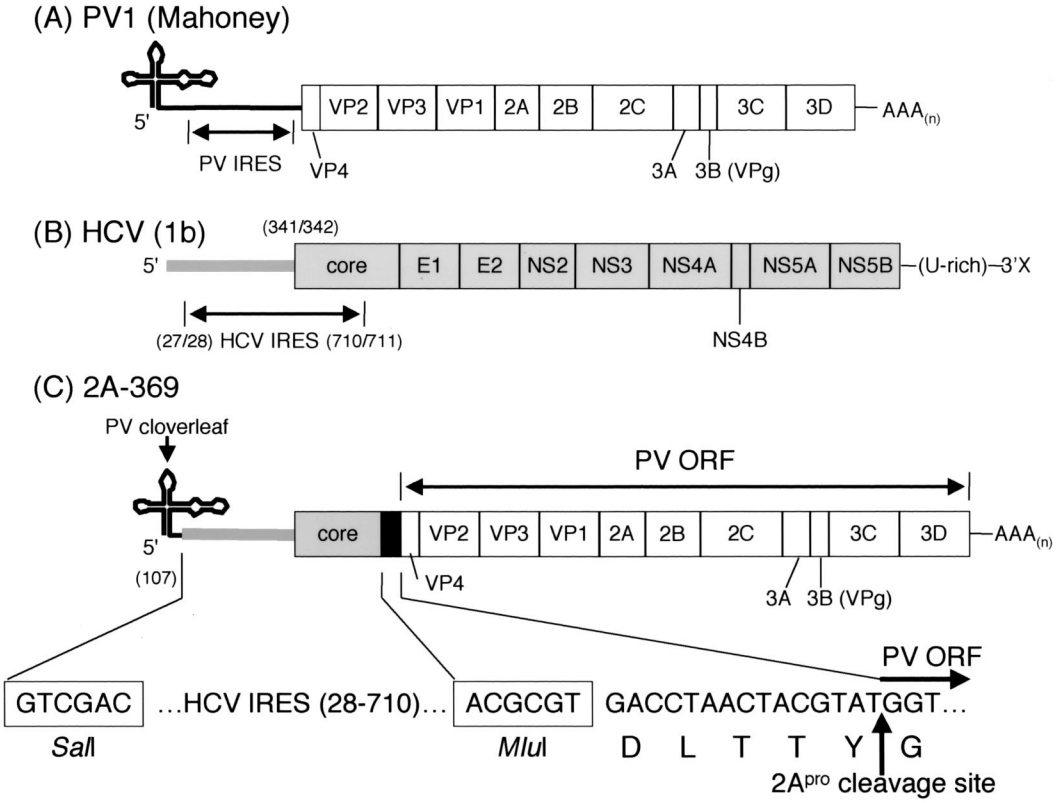

FIG. 3. Structures of viral genomes. Genome organizations of PV1 Mahoney (A), HCV genotype 1b (B), and the chimeric virus 2A-369 (C) are shown. Numbers in parentheses represent nucleotide numbers from the 5′ end of PV or HCV genome. The HCV IRES region, the $2A^{pro}$ cleavage site coding sequence, and restriction cleavage sites for *Sal*I and *Mlu*I in the genome of the 2A-369 virus are shown at the bottom of the figure. The cloverleaf-like RNA structure of PV is located at the 5′ end of the 2A-369 genome.

expression levels of hPVR in the liver. In fact, hPVR and its mRNA were not detected in the mouse liver by Western and Northern blotting, respectively (16). Preliminary experiments involving PVRTg21 revealed difficulties to obtain reproducible results in regard to replicating capacity of PV and its chimera 2A-369 (data not shown). New animal models are needed in order to proceed with these experiments.

MPH was initially discovered as mouse PVR homolog (24) and turned out later to be mouse PRR2 homolog (5). The expression level of MPH in the mouse liver is high, and its tissue distribution pattern in mice is more similar to that of hPVR in humans than that of hPVR in mice (2, 7, 16, 24). These observations led us to construct a fusion transgene consisting of the MPH regulatory gene and hPVR structural gene in order to generate a new Tg mouse model for poliomyelitis that possibly shows a tissue distribution pattern of hPVR similar to that in humans. The construction procedure of a MPVR fusion gene is described in Materials and Methods and is shown in Fig. 1. This fusion gene carries the MPH upstream sequence of ca. 12 kbp, which contains the 5′ portion of MPH cDNA reported by Morrison and Racaniello (24), and does not contain the ORF sequence of MPH mRNA.

Four lines of Tg mice derived from strain C57BL/6 have been established as described in Materials and Methods. Among them, MPVRTg25-61 was used in the present study. Southern blot hybridization was carried out to detect the transgene in the Tg mouse, MPVRTg25-61 (Fig. 2A). The pattern of radioactive bands (lane 1) detected in the *Bam*HI digests of the liver DNA of MPVRTg25-61 was identical with that of a fusion MPVR cosmid (lane 5). No band was detected in the DNA digests of the liver of littermates with no transgene (lane 2). From the intensity of radioactivity shown in Fig. 2A, the copy number of the transgene in MPVRTg25-61 appears to be ~40-fold that in HeLa S3 cells.

Detection of hPVR in various tissues. Expression of the MPVR fusion gene was investigated in the brain, spinal cord, liver, and small intestine of MPVRTg25-61 by Western blot analysis, and the expression pattern was compared to that of PVRTg21. As shown in Fig. 2B, ca. 70-kDa band was observed in the brain and spinal cord of MPVRTg25-61, and bands migrating to a position larger than 70 kDa were seen in the liver and small intestine of the Tg mice. This phenomenon might result from various degrees of glycosylation specific to these tissues. It is known that there are eight putative N-linked glycosylation sites in the extracellular domain of hPVR. Therefore, it is reasonable that they migrate to positions of molecular masses of 70 to 80 kDa, although molecular masses of protein moieties of membrane-bound form of hPVR (hPVRα and hPVRδ) are calculated to be 45 and 43 kDa, respectively (17). Anyway, we succeeded to generate new Tg mice that show hPVR expression both in the liver and in the brain.

Construction of 2A-369. A viable PV chimera (2A-369), in which the PV IRES was replaced by the HCV 5′UTR (nt 28 to 341) plus HCV ORF (nt 342 to 710), was constructed as de-

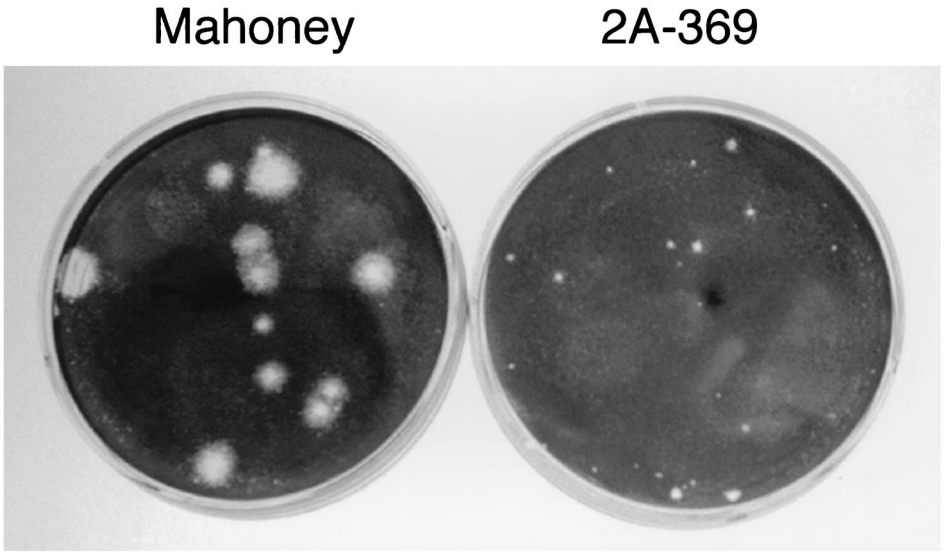

FIG. 4. Plaque size of 2A-369 virus. Plaques of Mahoney virus and 2A-369 virus on HeLa S3 cells are shown. HeLa cells were infected with viruses and incubated in medium containing 1% NCS and 1% agar at 36°C for 72 h. Infected cells were stained with 1% crystal violet in ethanol to visualize plaques.

scribed in Materials and Methods (Fig. 3). Nucleotide sequence for PV $2A^{pro}$ cleavage site was inserted at the junction of HCV sequence and PV ORF (Fig. 3). The 5′-cloverleaf-like RNA structure of PV, an essential *cis*-acting element for the RNA replication, was left as it is in the 2A-369 genome. Thus, the genome structure of 2A-369 is similar to that of P/H701-2A (41).

HeLa cells transfected with RNA derived from plasmid p2A-369 produced virus 2A-369. The plaque size of virus 2A-369 is much smaller than that of the parental Mahoney virus (Fig. 4). When the virus 2A-369 was passaged in HeLa cells at 37°C in DMEM containing 5% NCS, mutants with larger plaques easily emerged. To prevent the emergence of large plaque variants, HeLa cells after the RNA transfection were cultured at 36°C in DMEM containing 1% NCS. In this condition, the plaque size of 2A-369 remained small even after several passages in cultured cells.

Virus growth in the liver of MPVRTg25-61. To investigate virus replication in the liver, 10^4 PFU of Mahoney virus or 2A-369 virus were inoculated into the liver of MPVRTg25-61 mice or non-Tg C57BL/6 mice. The livers were removed from mice at 0, 12, 24, and 48 hpi and homogenized as described in Materials and Methods. The virus titers were measured by plaque assay (Fig. 5). In non-Tg mice, virus titers of both Mahoney and 2A-369 viruses did not increase up to 48 hpi. In MPVRTg25-61, however, titers of both viruses increased similarly with time up to 48 hpi. Large plaque variants of 2A-369 virus were not observed in virus preparation recovered from the infected liver. The data indicate that both viruses are able to multiply in the liver of MPVRTg25-61 mice. Titers of circulating virus at 0, 12, 24, and 48 hpi were also measured and were found to be negligible compared to titers of the virus recovered from the liver (data not shown). These results suggest that both IRESs of PV and HCV are active in the mouse liver.

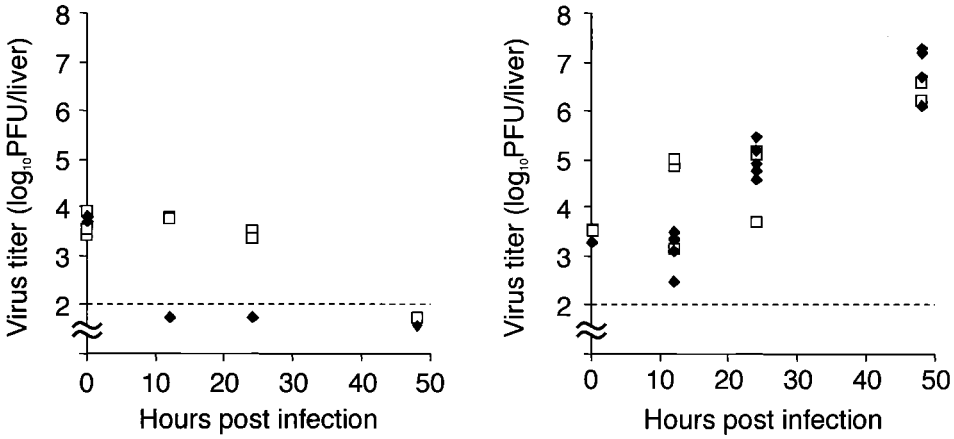

FIG. 5. Time course of virus titers in the liver after virus inoculation. The livers of MPVRTg25-61 mice (right panel) and C57BL/6 (non-Tg) mice (left panel) were inoculated with 10^4 PFU of Mahoney virus (□) or 2A-369 virus (◆). The virus titers in the liver at indicated times were measured as described in Materials and Methods and plotted. At each experimental condition, at least five mice were used.

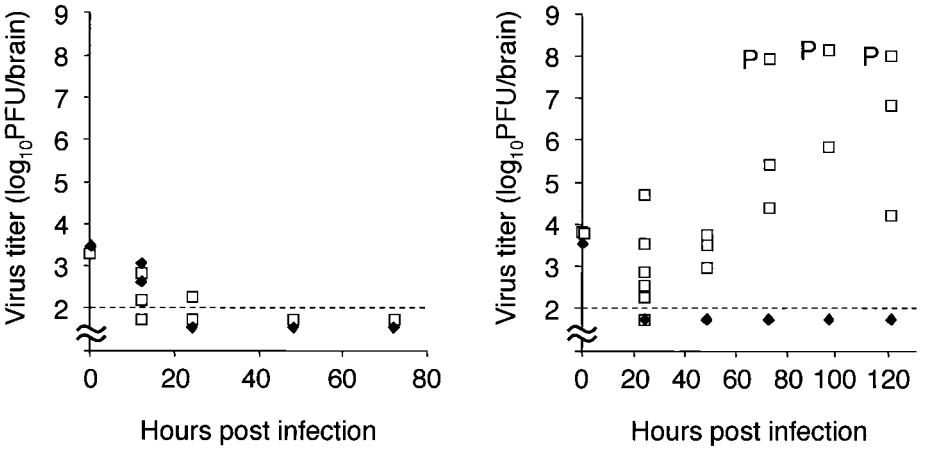

FIG. 6. Time course of virus titers in the brain after virus inoculation. MPVRTg25-61 mice (right panel) and C57BL/6 (non-Tg) mice (left panel) were intracerebrally inoculated with Mahoney virus (□) or 2A-369 virus (◆). Virus titers in the brain at the indicated times were measured as described in Materials and Methods and plotted. At each experimental condition, at least three mice were used. "P" in the figure indicates a paralyzed mouse.

Virus growth in the brain of MPVRTg25-61. MPVRTg25-61 or non-Tg mice were intracerebrally inoculated with 10^4 PFU of Mahoney or 2A-369 virus to examine the replicating capacity of these viruses in the brain (Fig. 6). At 0, 12, 24, 48, 72, 96, and 120 hpi, the brains were homogenized, and the virus titers were measured by plaque assay as described in Materials and Methods. Titers of both viruses in the brain of non-Tg mice did not increase up to 72 hpi. In the brain of MPVRTg25-61, titer of Mahoney virus increased, and some infected mice showed paralysis as expected (Fig. 6). Neurovirulence tests revealed that all of the mice intracerebrally inoculated with Mahoney virus died by 8 days after the inoculation (Fig. 7). Titer of 2A-369 virus in the brain of MPVRTg25-61, however, decreased with time after the inoculation (Fig. 6). No mice intracerebrally inoculated with 2A-369 virus died up to 14 days (Fig. 7). Thus, 2A-369 is not a neurovirulent virus. These data suggest that PV IRES efficiently works but HCV IRES hardly works in the brain of MPVRTg25-61.

PV antigens in the inoculated tissues. To confirm that PV Mahoney virus or the related 2A-369 virus multiply in the inoculated tissues of MPVRTg25-61, the brains and livers of the mice inoculated with 10^4 PFU of Mahoney or 2A-369 virus were examined for the presence of PV antigens. The frozen sections of the brain (cortex) and liver were prepared at 96 hpi and immunostained with rabbit anti-PV1 hyperimmune serum, followed by the reaction with fluorescein isothiocyanate-conjugated second antibody (Fig. 8).

In non-Tg mice inoculated with either of Mahoney or 2A-369 virus, the PV antigens were not detected in the sections of both the brain and liver. In MPVRTg25-61 mice inoculated with Mahoney virus, the antigens of PV were detected both in the brain and liver, whereas in the Tg mice inoculated with 2A-369 virus, PV antigens were detected only in the liver but not in the brain. These results are compatible with the results of virus titration experiments.

DISCUSSION

Expression of hPVR mRNA was detected in many human tissues, and the expression levels were relatively high in the liver and small intestine (7, 16). However, the hPVR mRNA was not detected in the liver and small intestine of PVRTg21 mice (Fig. 2B) and ICR-PVRTg1 mice (16). A similar observation was reported by Ren and Racaniello (30). Thus, the expression pattern of hPVR mRNA in mice is greatly different from that in humans. The regulation mechanisms of the hPVR gene introduced in mice may not be the same as those in humans. The *cis*-acting elements on hPVR gene may not function properly in mice, or the transgene may not contain all of the *cis*-acting elements.

The expression pattern of MPH mRNA in mice reported by Morrison and Racaniello (24) was similar to that of hPVR mRNA in humans (16). To obtain the human-type expression pattern of hPVR mRNA in mice, the hPVR upstream sequence of ca. 11 kbp in cosmid HC5 possibly containing regulatory elements was replaced by the MPH upstream sequence of ca. 12 kbp in the present study. This new transgene conferred hPVR expression to the liver and small intestine, as well

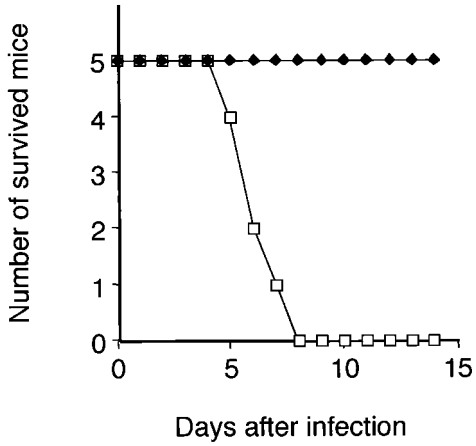

FIG. 7. Mouse neurovirulence test. MPVRTg25-61 mice were intracerebrally inoculated with 10^4 PFU of Mahoney virus (□) or 2A-369 virus (◆). The infected mice were observed for paralysis and mortality every 24 h for up to 14 days.

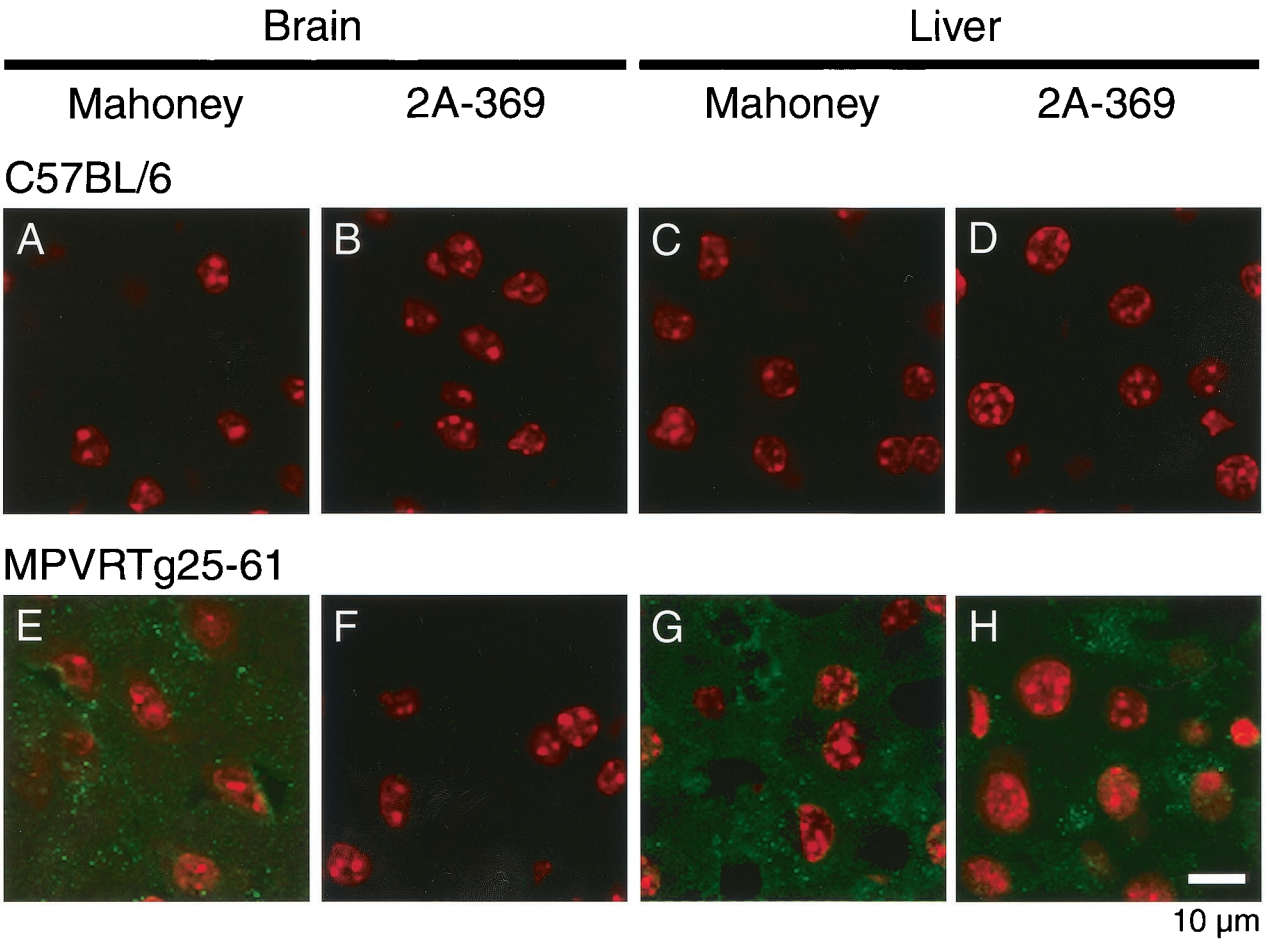

FIG. 8. PV antigens in the inoculated tissues. Into the brain (A, B, E, and F) or liver (C, D, G, and H) of MPVRTg25-61 (E to H) or C57BL/6 (non-Tg) (A to D), 10^4 PFU of Mahoney virus (A, C, E, and G) or 2A-369 virus (B, D, F, and H) were inoculated. The tissue sections were prepared 96 hpi, and the frozen sections were immunostained as described in Materials and Methods. Red represents nucleic acids, and green represents PV antigens. A scale bar (10 μm) is indicated in panel H.

as to the brain and spinal cord (Fig. 2B). The expression level in the liver, however, was lower than expected compared to those in other tissues and higher in the brain. This indicates that the new transgene still does not contain all of the *cis*-acting elements. It has been reported that distant regulatory sequences are required for high-level expression of certain genes, such as the globin genes (28).

Although the threshold of hPVR expression to give susceptibility to cells is not known at present, the liver cells of MPVRTg25-61 are susceptible to PV and the related chimera 2A-365 virus (see Fig. 5 and 8). Interestingly, high-level expression of hPVR gene was observed in the small intestine of MPVRTg25-61 mice. However, this new mouse model showed very low susceptibility to oral administration of PV (data not shown). This phenomenon is compatible with the observation reported by Zhang and Racaniello (40).

The small-plaque phenotype of virus 2A-369 appeared to be unstable, and variants with larger-plaque phenotypes were ready to emerge during passaging through HeLa S3 cells at 37°C. This instability of plaque phenotype was successfully repressed up to several passages by incubating infected HeLa cells at 36°C in DMEM containing 1% NCS. Virus yield of 2A-369 in a single cycle infection by 10 hpi was about a tenth part of that of Mahoney virus in HeLa cells (data not shown). The eclipse phase of 2A-369 lasted for 4 h after infection of HeLa cells, whereas that of Mahoney virus lasted for 2 h (data not shown). These results are compatible with the observation of the small-plaque phenotype of 2A-369 virus. The virus yield and duration of eclipse state of 2A-369 are similar to those of P/H701-2A (41). In the same way as P/H701-2A, production of the HCV core protein moiety would not be necessary for the translation and replication of the 2A-369.

Several *cis*-acting elements of viral RNA replication were suggested to reside within PV IRES. Borman et al. (4) suggested that the RNA segment (ca. nt 343 to 500) within the IRES controls viral RNA synthesis. Shiroki et al. (32) identified nt 133 to be a *cis*-acting element for RNA replication. Therefore, replacement of PV IRES by HCV IRES may affect RNA replication mechanisms of 2A-369. This may modify the virus replication process of 2A-369 in the liver and brain of MPVRTg25-61. However, it is reasonable that HCV IRES works in the liver, resulting in virus replication of 2A-369 in the liver of MPVRTg25-61.

It is of interest that Mahoney virus, as well as 2A-369 virus,

replicates in the liver, indicating that PV IRES is also active in cells of the mouse liver. In humans, a high-level expression of hPVR was evident in the liver (7, 16). Nevertheless, the human liver is not considered to be a replication site of PV. These observations suggest that the susceptibility of tissues to PV is not only determined by the distribution of hPVR and IRES activity. There may be differences in the host factors that support PV IRES activity in the liver between humans and mice. Unknown interactions between PV and host cells that determine PV susceptibility may exist. This unknown interaction must be clarified in order to understand fully the molecular mechanisms of PV pathogenicity. Alternatively, innate immunity system may protect tissues other than the CNS against PV infection. In fact, virus titers of both Mahoney and 2A-369 viruses in the liver of MPVRTg25-61 begin to decrease on the third day of infection (data not shown).

Our data in the present study strongly suggest that tissue-specific activity of IRES on viral RNAs is an important determinant of tissue tropism of the virus. Thus, study of viral IRESs appears to be essential for understanding the viral pathogenesis. Considering that many cellular IRESs have been discovered and that individual cellular IRESs are different in their RNA structures, these IRESs may also be active only in specific conditions depending on their RNA structures. Cellular proteins driven by cellular IRES elements may be translated in cell-specific, tissue-specific, developmental-stage-specific, cell cycle-specific, and physiological-condition (virus infection, heat shock, etc.)-specific manners. Thus, cellular IRESs may be important *cis*-acting elements for regulate gene expression in the posttranscriptional stage.

ACKNOWLEDGMENTS

We thank Satoshi Koike and Junken Aoki for encouragement and valuable discussions during the course of this study and Etsuko Suzuki and Yuri Matsushita for help in preparing the manuscript.

This work was supported by a Grant-in-Aid for Specially Promoted Research from the Ministry of Education, Science, Sports, and Culture of Japan.

REFERENCES

1. **Andino, R., G. E. Rieckhof, P. L. Achacoso, and D. Baltimore.** 1993. Poliovirus RNA synthesis utilizes an RNP complex formed around the 5′-end of viral RNA. EMBO J. **12:**3587–3598.
2. **Aoki, J., S. Koike, H. Asou, I. Ise, H. Suwa, T. Tanaka, M. Miyasaka, and A. Nomoto.** 1997. Mouse homolog of poliovirus receptor-related gene 2 product, mPRR2, mediates homophilic cell aggregation. Exp. Cell Res. **235:**374–384.
3. **Arita, M., S. Koike, J. Aoki, H. Horie, and A. Nomoto.** 1998. Interaction of poliovirus with its purified receptor and conformational alteration in the virion. J. Virol. **72:**3578–3586.
4. **Borman, A. M., F. G. Deliat, and K. M. Kean.** 1994. Sequences within the poliovirus internal ribosome entry segment control viral RNA synthesis. EMBO J. **13:**3149–3157.
5. **Eberle, F., P. Dubreuil, M. G. Mattei, E. Devilard, and M. Lopez.** 1995. The human PRR2 gene, related to the human poliovirus receptor gene (PVR), is the true homolog of the murine MPH gene. Gene **159:**267–272.
6. **Evans, D. M., G. Dunn, P. D. Minor, G. C. Schild, A. J. Cann, G. Stanway, J. W. Almond, K. Currey, and J. V. Maizel, Jr.** 1985. Increased neurovirulence associated with a single nucleotide change in a noncoding region of the Sabin type 3 poliovaccine genome. Nature **314:**548–550.
7. **Freistadt, M. S., G. Kaplan, and V. R. Racaniello.** 1990. Heterogeneous expression of poliovirus receptor-related proteins in human cells and tissues. Mol. Cell. Biol. **10:**5700–5706.
8. **Gromeier, M., L. Alexander, and E. Wimmer.** 1996. Internal ribosomal entry site substitution eliminates neurovirulence in intergeneric poliovirus recombinants. Proc. Natl. Acad. Sci. USA **93:**2370–2375.
9. **Gromeier, M., B. Bossert, M. Arita, A. Nomoto, and E. Wimmer.** 1999. Dual stem-loops within the poliovirus internal ribosomal entry site control neurovirulence. J. Virol. **73:**958–964.
10. **Horie, H., S. Koike, T. Kurata, Y. Sato-Yoshida, I. Ise, Y. Ota, S. Abe, K. Hioki, H. Kato, and C. Taya.** 1994. Transgenic mice carrying the human poliovirus receptor: new animal models for study of poliovirus neurovirulence. J. Virol. **68:**681–688.
11. **Isoyama, T., N. Kamoshita, K. Yasui, A. Iwai, K. Shiroki, H. Toyoda, A. Yamada, Y. Takasaki, and A. Nomoto.** 1999. Lower concentration of La protein required for internal ribosome entry on hepatitis C virus RNA than on poliovirus RNA. J. Gen. Virol. **80:**2319–2327.
12. **Jang, S. K., H. G. Krausslich, M. J. Nicklin, G. M. Duke, A. C. Palmenberg, and E. Wimmer.** 1988. A segment of the 5′ nontranslated region of encephalomyocarditis virus RNA directs internal entry of ribosomes during in vitro translation. J. Virol. **62:**2636–2643.
13. **Kamoshita, N., K. Tsukiyama-Kohara, M. Kohara, and A. Nomoto.** 1997. Genetic analysis of internal ribosomal entry site on hepatitis C virus RNA: implication for involvement of the highly ordered structure and cell type-specific transacting factors. Virology **233:**9–18.
14. **Kato, N., M. Hijikata, Y. Ootsuyama, M. Nakagawa, S. Ohkoshi, T. Sugimura, and K. Shimotohno.** 1990. Molecular cloning of the human hepatitis C virus genome from Japanese patients with non-A, non-B hepatitis. Proc. Natl. Acad. Sci. USA **87:**9524–9528.
15. **Kawamura, N., M. Kohara, S. Abe, T. Komatsu, K. Tago, M. Arita, and A. Nomoto.** 1989. Determinants in the 5′ noncoding region of poliovirus Sabin 1 RNA that influence the attenuation phenotype. J. Virol. **63:**1302–1309.
16. **Koike, S., J. Aoki, and A. Nomoto.** 1994. Transgenic mouse for the study of poliovirus pathogenicity, p. 463–480. *In* E. Wimmer (ed.), Cellular receptors for animal viruses. Cold Spring Harbor Laboratory Press, Cold Spring Harbor, N.Y.
17. **Koike, S., H. Horie, I. Ise, A. Okitsu, M. Yoshida, N. Iizuka, K. Takeuchi, T. Takegami, and A. Nomoto.** 1990. The poliovirus receptor protein is produced both as membrane-bound and secreted forms. EMBO J. **9:**3217–3224.
18. **Koike, S., C. Taya, T. Kurata, S. Abe, I. Ise, H. Yonekawa, and A. Nomoto.** 1991. Transgenic mice susceptible to poliovirus. Proc. Natl. Acad. Sci. USA **88:**951–955.
19. **Kolykhalov, A. A., S. M. Feinstone, and C. M. Rice.** 1996. Identification of a highly conserved sequence element at the 3′ terminus of hepatitis C virus genome RNA. J. Virol. **70:**3363–3371.
20. **Krausslich, H. G., and E. Wimmer.** 1988. Viral proteinases. Annu. Rev. Biochem. **57:**701–754.
21. **Lu, H. H., and E. Wimmer.** 1996. Poliovirus chimeras replicating under the translational control of genetic elements of hepatitis C virus reveal unusual properties of the internal ribosomal entry site of hepatitis C virus. Proc. Natl. Acad. Sci. USA **93:**1412–1417.
22. **Macadam, A. J., S. R. Pollard, G. Ferguson, G. Dunn, R. Skuce, J. W. Almond, and P. D. Minor.** 1991. The 5′ noncoding region of the type 2 poliovirus vaccine strain contains determinants of attenuation and temperature sensitivity. Virology **181:**451–458.
23. **Miyamura, T., and Y. Matsuura.** 1993. Structural proteins of hepatitis C virus. Trends Microbiol. **1:**229–231.
24. **Morrison, M. E., and V. R. Racaniello.** 1992. Molecular cloning and expression of a murine homolog of the human poliovirus receptor gene. J. Virol. **66:**2807–2813.
25. **Ohka, S., W. X. Yang, E. Terada, K. Iwasaki, and A. Nomoto.** 1998. Retrograde transport of intact poliovirus through the axon via the fast transport system. Virology **250:**67–75.
26. **Omata, T., M. Kohara, S. Kuge, T. Komatsu, S. Abe, B. L. Semler, A. Kameda, H. Itoh, M. Arita, E. Wimmer, and A. Nomoto.** 1986. Genetic analysis of the attenuation phenotype of poliovirus type 1. J. Virol. **58:**348–358.
27. **Pelletier, J., and N. Sonenberg.** 1988. Internal initiation of translation of eukaryotic mRNA directed by a sequence derived from poliovirus RNA. Nature **334:**320–325.
28. **Peterson, K. R., Q. L. Li, C. H. Clegg, T. Furukawa, P. A. Navas, E. J. Norton, T. G. Kimbrough, and G. Stamatoyannopoulos.** 1995. Use of yeast artificial chromosomes (YACs) in studies of mammalian development: production of beta-globin locus YAC mice carrying human globin developmental mutants. Proc. Natl. Acad. Sci. USA **92:**5655–5659.
29. **Pilipenko, E. V., E. G. Viktorova, S. T. Guest, V. I. Agol, and R. P. Roos.** 2001. Cell-specific proteins regulate viral RNA translation and virus-induced disease. EMBO J. **20:**6899–6908.
30. **Ren, R., and V. R. Racaniello.** 1992. Human poliovirus receptor gene expression and poliovirus tissue tropism in transgenic mice. J. Virol. **66:**296–304.
31. **Reynolds, J. E., A. Kaminski, H. J. Kettinen, K. Grace, B. E. Clarke, A. R. Carroll, D. J. Rowlands, and R. J. Jackson.** 1995. Unique features of internal initiation of hepatitis C virus RNA translation. EMBO J. **14:**6010–6020.
32. **Shiroki, K., T. Ishii, T. Aoki, M. Kobashi, S. Ohka, and A. Nomoto.** 1995. A new *cis*-acting element for RNA replication within the 5′ noncoding region of poliovirus type 1 RNA. J. Virol. **69:**6825–6832.
33. **Takahashi, K., H. Nakanishi, M. Miyahara, K. Mandai, K. Satoh, A. Satoh, H. Nishioka, J. Aoki, A. Nomoto, A. Mizoguchi, and Y. Takai.** 1999. Nectin/PRR: an immunoglobulin-like cell adhesion molecule recruited to cadherin-based adherens junctions through interaction with Afadin, a PDZ domain-containing protein. J. Cell Biol. **145:**539–549.

34. **Takamizawa, A., C. Mori, I. Fuke, S. Manabe, S. Murakami, J. Fujita, E. Onishi, T. Andoh, I. Yoshida, and H. Okayama.** 1991. Structure and organization of the hepatitis C virus genome isolated from human carriers. J. Virol. **65:**1105–1113.
35. **Tanaka, T., N. Kato, M. J. Cho, K. Sugiyama, and K. Shimotohno.** 1996. Structure of the 3′ terminus of the hepatitis C virus genome. J. Virol. **70:**3307–3312.
36. **Tsukiyama-Kohara, K., N. Iizuka, M. Kohara, and A. Nomoto.** 1992. Internal ribosome entry site within hepatitis C virus RNA. J. Virol. **66:**1476–1483.
37. **Vagner, S., B. Galy, and S. Pyronnet.** 2001. Irresistible IRES. Attracting the translation machinery to internal ribosome entry sites. EMBO Rep. **2:**893–898.
38. **Wang, C., P. Sarnow, and A. Siddiqui.** 1993. Translation of human hepatitis C virus RNA in cultured cells is mediated by an internal ribosome-binding mechanism. J. Virol. **67:**3338–3344.
39. **Yang, W. X., T. Terasaki, K. Shiroki, S. Ohka, J. Aoki, S. Tanabe, T. Nomura, E. Terada, Y. Sugiyama, and A. Nomoto.** 1997. Efficient delivery of circulating poliovirus to the central nervous system independently of poliovirus receptor. Virology **229:**421–428.
40. **Zhang, S., and V. R. Racaniello.** 1997. Expression of the poliovirus receptor in intestinal epithelial cells is not sufficient to permit poliovirus replication in the mouse gut. J. Virol. **71:**4915–4920.
41. **Zhao, W. D., E. Wimmer, and F. C. Lahser.** 1999. Poliovirus/hepatitis C virus (internal ribosomal entry site-core) chimeric viruses: improved growth properties through modification of a proteolytic cleavage site and requirement for core RNA sequences but not for core-related polypeptides. J. Virol. **73:** 1546–1554.